Constitutive model for fiber-reinforced materials with deformable matrices

J. Planas, G. V. Guinea, and M. Elices
Departamento Ciencia de Materiales, Universidad Politécnica de Madrid,
ETSI Caminos, c/ Prof. Aranguren s/n, ES28040-Madrid, Spain
(Received 24 May 2007; revised manuscript received 18 July 2007; published 4 October 2007)

A great number of biological structures are composed of fibers (elastin, collagen, etc.) dispersed on an aqueous matrix in such a complex way that a detailed mechanical analysis based on microconstituents is, for practical purposes, out of reach. Consequently, the preferred approach to the mechanical behavior of these materials is based on setting up of constitutive equations that homogenize the behavior while capturing their main microstructural features. This work presents a simple macroscopic model for fiber-reinforced materials with deformable matrices, especially suited to many biological structural tissues. The constitutive equation is derived by imposing equivalence between the virtual works of both the fiber-reinforced and the equivalent continuum media, showing that it is independent of the control volume used for such equivalence. The model is particularized to incompressible materials, and an extension to orthotropic biological fibers is shown. Numerical simulations of uniaxial tests on silk fibers demonstrate the model's ability to capture the progressive alignment of the microconstituents under large deformations.

DOI: 10.1103/PhysRevE.76.041903 PACS number(s): 87.16.Ac, 62.20.−x, 81.40.Jj, 46.05.+b

I. INTRODUCTION

There is a growing interest in understanding the mechanical behavior of fiber composites with highly deformable matrices. Most biological structural components are composites based on a fluidlike matrix and fibers (collagen, elastin, fibroin, etc.). The attractiveness lies not only in solving the involved problem of structure-property relations, but in the power of biomimetism; if the effect of micromechanisms on macroscopic properties can be unveiled, these properties can be enhanced by modifying the properties of fibers and matrices.

Several approaches have been presented for studying the micromechanics of biological fiber composites, such approaches depending to a large extent on the information being sought after. Scientists working on the structural mechanics of such complex systems are drawn in two opposing directions.

(i) *Macroscopic models* for the description of the continuous media where mechanical analysis requires simplification and properties are randomized or, when making use of macroscopic parameters, they commonly lack physical meaning and, more often than not, are coupled. The constitutive equations for these models are developed in general using two different approaches, with each based on a different viewpoint, either molecular or continuum.

The molecular viewpoint introduces microstructural elements, usually with chain configuration, that represent single macromolecules or other microscopical units. The freely jointed chain [1] and wormlike chain [2] models are typically used to evaluate the behavior of individual chains that are assembled into three-dimensional networks via a discrete spatial representation (like three-chain [3] and eight-chain models [4]) or by a continuous distribution (full-chain model [5]). Finally, the macroscopic constitutive equation is derived from multichain assemblies [6]. Such an approach has been recently used to propose a model for cytoskeletal networks, natural fibers, and soft biological tissues [7].

Hierarchical models can be included within the molecular viewpoint since they build the macroscopic assembly from microscopic units, but they use a different strategy. Modules of the same hierarchical level assemble to produce a supramodule (i.e., a module of the next higher complexity level) in a merging process up to the whole structure. Interactions between modules at the same hierarchical level are assembled to obtain the response function of the corresponding supramodule, which, in turn, is used to build the response of the next-level supramodule. To moderate the increasing complexity of higher levels, hierarchical models usually concentrate on a reduced set of parameters (for example, force and extension) that are modeled by simple explicit relationships at the deepest levels [8].

The continuum viewpoint makes a phenomenological approach to the macroscopic behavior by introducing constitutive equations whose parameters are fitted to the experimental data. Constitutive equations for soft biological materials have been developed within the finite-strain framework by Fung and other researchers (see, for example, [9,10] and references therein), with most using polynomial expansions of the strain invariants with a large number of fit parameters.

To circumvent the incorporation of a large number of material parameters, especially in order to model the anisotropic behavior of fiber-reinforced tissues, Holzapfel and coworkers [11] have explicitly introduced the fiber geometry in the constitutive equation by means of the specific invariants, within the framework proposed by Spencer [12]. Nevertheless, the benefits of the reduction of material parameters are balanced by a severe increase in computational difficulty. In addition, the problem of physical identification of material parameters remains unsolved.

(ii) *Microscopic models* aiming at reflecting the complex reality are usually very involved, not only due to the huge amount of parameters, but also to the difficulty in implementing numerical computations. Models for biological fibers usually descend into the nanometer scale, requiring elusive information about the molecular network like mechanical properties of different chemical bonds [13] or mor-

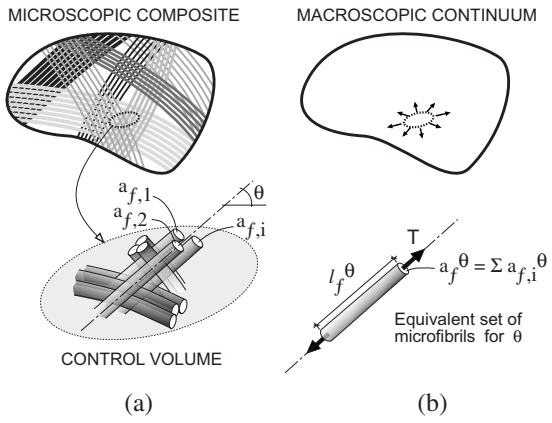

FIG. 1. Composite material and continuum equivalent.

phological structure [14]. Notwithstanding that these models help to understand the role of basic molecular and supramolecular units, their results are still far away from being applicable to arbitrary macroscopic configurations [15,16].

The purpose of this paper is to present a simple macroscopic continuum model with deep insight into the physical meaning, as it considers fiber realignment during matrix deformation. This goal is achieved by means of the constitutive equation of the microfibril, where the relevant aspects and parameters are selected. The model naturally integrates the relevant microfibril properties and the macroscopic continuum behavior in a simple formulation applicable to any macroscopic situation and uses a reduced set of parameters, all with physical significance. The continuum model presented in this paper aims at filling the existing gap between the involved (and limited) micromolecular models and macroscopic phenomenological models without resorting to unrealistic assumptions or unphysical parameters.

The paper is structured as follows: First, the model is justified by forcing the continuum to give the same mechanical dissipation as the fiber-reinforced material under any arbitrary motion. The second section deals with the particularization of the model for incompressible materials. The paper closes with an application of the model to tensile stretching of silk fibers, where anisotropy, strong nonlinearity, and microfibril alignment during different mechanical loading were considered and were found to agree largely with experimental measurements.

II. MODEL

A. Introduction and objective

A great number of fiber-reinforced materials, either natural or artificial, can be accurately described as a composite consisting of a deformable matrix with one or more sets of filaments embedded [Fig. 1(a)]. For these materials, most of their mechanical performance is due to the progressive alignment and recruitment upon straining of their constituent microfibrils and, consequently, any realistic macroscopic approach should take into account this strengthening mechanism and its dependence on the deformed geometry.

The purpose of this paper is to establish a macroscopic model, capable of reproducing the mechanical response of the involved fiber-reinforced material, without dealing with mesoscopic details during every loading step. The mechanics of continuous media provides the appropriate framework for dealing with problems like the one mentioned above, since it naturally deals with large deformations and provides sound measurements for stress and strain.

For this purpose an equivalent continuum macroscopic model for fiber-reinforced materials with perfectly deformable matrices is derived by forcing the model to give the same mechanical dissipation as the fiber-reinforced material under any arbitrary motion. To this end, the mechanical power of forces acting on the fiber composite under a given deformation is first computed, and this value is used to deduce the stress tensor that would produce the same rate of work for the motion.

B. Fiber-reinforced material

The actual material is assumed to consist of sets of microfibrils dispersed into a deformable matrix in such a way that microfibrils can be considered continuous and straight through any sufficiently small *control volume*, like the one illustrated in Fig. 1. We also assume that no force is transmitted through the matrix in the composite material—i.e., that the matrix is perfectly deformable and forces only build up in the microfibrils as a consequence of deformation. In the initial configuration, taken as reference, materials are unstressed.

With reference to the control volume in Fig. 1 and according to the hypotheses stated above, the only forces acting on it are the forces on the microfibrils.

The mechanical power of the instant force T acting on a given set of microfibrils of length l_f in the current (instant, deformed) configuration is $T\dot{l}_f$, where the overdot refers to time derivation, and its ratio per unit volume of microfibrils in the current configuration can be computed as

$$\frac{T\dot{l}_f}{a_f l_f} = \frac{T\dot{\lambda}_f}{a_f \lambda_f}, \tag{1}$$

where a_f is the current cross section of the microfibrils and λ_f the stretching, given by

$$\lambda_f = \frac{l_f}{L_f}, \tag{2}$$

with L_f being the length of the microfibrils in the reference (initial, unstressed) configuration.

The mechanical power per unit volume of composite material is easily obtained by multiplying Eq. (1) by f, the microfibrils volume fraction, assumed constant at a given (material) point during the deformation:

$$\frac{T\dot{\lambda}_f}{a_f \lambda_f} f. \tag{3}$$

In the referential description, Eq. (3) becomes

$$\frac{f}{J}\dot{\lambda}_f s_f, \tag{4}$$

where we have introduced s_f, the nominal stress in the microfibrils, defined as

$$s_f = \frac{T}{A_f}, \tag{5}$$

and made use of the fact that the current volume $a_f l_f$ is equal to $JA_f L_f$, A_f being the initial cross section and

$$J = \det \mathbf{F} \tag{6}$$

the determinant of $\mathbf{F}$, the deformation gradient that connects the reference and the current configuration. Labeling $\mathbf{x}$ and $\mathbf{X}$ the position vectors in the current and reference configurations, respectively, $\mathbf{F}$ is given by

$$\mathbf{F} = \text{grad}\,\mathbf{x}, \tag{7}$$

where "grad" is the gradient operator with respect to $\mathbf{X}$.

The stretching in the microfibril, λ_f, can be expressed as a function of $\mathbf{F}$: namely [17],

$$\lambda_f = +\sqrt{\mathbf{C}\mathbf{N}\cdot\mathbf{N}}, \tag{8}$$

where $\mathbf{N}$ is the unit vector along the microfibril in the reference configuration and $\mathbf{C}=\mathbf{F}^{\mathrm{T}}\mathbf{F}$ the right Cauchy-Green strain tensor. Substitution of the time derivative of Eq. (8) into (4) yields

$$\frac{f s_f}{2J}\frac{\dot{\mathbf{C}}\mathbf{N}\cdot\mathbf{N}}{\sqrt{\mathbf{C}\mathbf{N}\cdot\mathbf{N}}} \tag{9}$$

and recalling that

$$\dot{\mathbf{C}}\mathbf{N}\cdot\mathbf{N} = \mathrm{tr}(\dot{\mathbf{C}}\mathbf{N}\otimes\mathbf{N}) = \mathrm{tr}[\dot{\mathbf{C}}(\mathbf{N}\otimes\mathbf{N})] = \mathrm{tr}[(\mathbf{N}\otimes\mathbf{N})\dot{\mathbf{C}}], \tag{10}$$

since the trace of the tensor product ($\otimes$) of two vectors is their dot product, we finally arrive, for the mechanical power per unit volume at a given set of microfibrils, in the referential description, at

$$\mathrm{tr}\left(\frac{f s_f}{2J\sqrt{\mathbf{C}\mathbf{N}\cdot\mathbf{N}}}(\mathbf{N}\otimes\mathbf{N})\dot{\mathbf{C}}\right). \tag{11}$$

The power done by forces acting on all sets of microfibrils across the control volume, each set referred by the index Θ (see Fig. 1), is computed by adding up their contributions:

$$P_f = \sum_\Theta \mathrm{tr}\left(\frac{f_f^\Theta s_f^\Theta}{2J\sqrt{\mathbf{C}\mathbf{N}_\Theta\cdot\mathbf{N}_\Theta}}(\mathbf{N}_\Theta\otimes\mathbf{N}_\Theta)\dot{\mathbf{C}}\right)$$

$$= \mathrm{tr}\sum_\Theta \frac{f_f^\Theta s_f^\Theta}{2J\sqrt{\mathbf{C}\mathbf{N}_\Theta\cdot\mathbf{N}_\Theta}}(\mathbf{N}_\Theta\otimes\mathbf{N}_\Theta)\dot{\mathbf{C}}. \tag{12}$$

Equation (12) gives the mechanical power per unit volume in the reference configuration of the forces acting on the control volume which, interestingly, has no more requirements on its size and shape than to enclose straight strands of microfibrils. Consequently, taking the smallest volume that meets the aforesaid condition as the control volume, Eq. (12), can be regarded as the mechanical power per unit volume at a given point.

C. Macroscopic continuum material

In the equivalent continuum model, the mechanical power per unit volume in the current configuration is ordinarily called the stress power, as shown, for example, in Ref. [17], and is computed via the equation

$$\mathrm{tr}(\boldsymbol{\sigma}\mathbf{D}), \tag{13}$$

where $\boldsymbol{\sigma}$ is the Cauchy stress tensor and $\mathbf{D}$ the symmetric part of the velocity gradient, $\mathbf{L}=\dot{\mathbf{F}}\mathbf{F}^{-1}$. The stress power referred to a unit volume in the reference configuration can be expressed as [17]

$$P_\sigma = \frac{1}{2}\mathrm{tr}(\mathbf{S}\dot{\mathbf{C}}), \tag{14}$$

where the second Piola-Kirchoff stress tensor $\mathbf{S}=J\mathbf{F}^{-1}\boldsymbol{\sigma}\mathbf{F}^{-\mathrm{T}}$ has been introduced.

D. Mechanical equivalence

The mechanical equivalence between the continuum model and the composite material is set by forcing $P_f=P_\sigma$ for all possible motions, with the help of Eqs. (12) and (14): i.e.,

$$\mathrm{tr}\left(\frac{1}{2}\mathbf{S}\dot{\mathbf{C}}\right) = \mathrm{tr}\sum_\Theta \frac{f_f^\Theta s_f^\Theta}{2J\sqrt{\mathbf{C}\mathbf{N}_\Theta\cdot\mathbf{N}_\Theta}}(\mathbf{N}_\Theta\otimes\mathbf{N}_\Theta)\dot{\mathbf{C}} \tag{15}$$

for any $\dot{\mathbf{C}}$.

The equivalence shown in Eq. (15) is a customary procedure to link the microscopic description of a physical system (right-hand side of the equation) and its corresponding macroscopic equivalent (left-hand side) while preserving the macroscopic mechanical power (stress power) dissipated or stored by the system [18,19]. This equivalence—presented in different forms—emerges in a number of problems related to molecular or microscopic models such as the statement of the stress tensor from the atomic or molecular interactions by application of the virial theorem, as shown, for example, in [20–22].

However, different from other approaches, Eq. (15) is based only on the constitutive behavior of microfibrils whose complex response is not modeled from molecular interactions, thus avoiding the usual assumptions in molecular dynamics (intermolecular potentials, time averages, and periodic systems). Particularly important is the fact that Eq. (15) applies without regard to whether the forces in the microfibrils are conservative or not, as is clearly illustrated in the application to silk fibers in the last section of this paper.

Fulfillment of Eq. (15) for any deformation process leads to the condition

$$\mathbf{S} = \sum_\Theta \frac{f_f^\Theta s_f^\Theta}{J\sqrt{\mathbf{C}\mathbf{N}_\Theta\cdot\mathbf{N}_\Theta}}(\mathbf{N}_\Theta\otimes\mathbf{N}_\Theta), \tag{16}$$

which gives the constitutive relationship for the equivalent model in terms of the second Piola-Kirchoff stress and the right Cauchy-Green strain tensors.

Equation (16) has to be complemented with the relationship between the nominal stress s_f^Θ and the elongation λ_f^Θ within the microfibrils,

$$s_f^\Theta = s_f^\Theta(\lambda_f^\Theta) = s_f^\Theta(\sqrt{\mathbf{C}\mathbf{N}_\Theta \cdot \mathbf{N}_\Theta}), \tag{17}$$

which supplies the micromechanical information to the model. As shown below in Sec. IV, the tensile behavior of individual microfibrils is described by means of Eq. (17), which can be adequately assembled to reveal the key micromechanisms that make up the mechanical behavior of the fiber-reinforced material.

Equations (16) and (17) completely define the constitutive relationship of the equivalent continuum model. It is worth remarking that Eq. (16) does not presume any given material behavior, either elastic, plastic, or time dependent, which is entirely controlled by the functional form of Eq. (17). Thus, Eq. (16) will account for geometrical changes induced during the deformational process like fiber orientation.

A possible extension to non-perfectly-deformable matrices can be readily implemented by introducing an extra term on the right-hand side of Eq. (15) to account for the stress power of the matrix. As an example, in the case of hyperelastic matrices (i.e., matrices with a strain energy function W) where the stress power can be expressed as $\mathrm{tr}[(\partial W/\partial \mathbf{C})\dot{\mathbf{C}}]$, Eq. (16) would have to be modified by adding the term $\partial W/\partial \mathbf{C}$ to its right-hand side.

III. PARTICULARIZATION FOR INCOMPRESSIBLE MATERIALS

The particularization of Eq. (16) to incompressible materials can be carried out by introduction of a Lagrange multiplier associated with the constraint

$$\frac{d}{dt}(\det \mathbf{C}) = 0, \tag{18}$$

which is derived directly from the condition of volume constancy $J=\sqrt{\det \mathbf{C}}=1$.

Equation (18) can be transformed to read

$$\frac{d}{dt}(\det \mathbf{C}) = \det \mathbf{C}\ \mathrm{tr}(\dot{\mathbf{C}}\mathbf{C}^{-1}) = \mathrm{tr}(\mathbf{C}^{-1}\dot{\mathbf{C}}) = 0 \tag{19}$$

and the mechanical equivalence, Eq. (15), is now given by

$$\mathrm{tr}\left(\frac{1}{2}\mathbf{S}\dot{\mathbf{C}}\right) = \mathrm{tr}\sum_\Theta \frac{f_f^\Theta s_f^\Theta}{2\sqrt{\mathbf{C}\mathbf{N}_\Theta \cdot \mathbf{N}_\Theta}}(\mathbf{N}_\Theta \otimes \mathbf{N}_\Theta)\dot{\mathbf{C}} - p^*\mathrm{tr}(\mathbf{C}^{-1}\dot{\mathbf{C}}) \tag{20}$$

for any $\dot{\mathbf{C}}$, p^* being the Lagrange multiplier.

The resulting stress tensor is then dependent on p^*, which represents an arbitrary hydrostatic pressure induced by the constraint

$$\mathbf{S} = \sum_\Theta \frac{f_f^\Theta s_f^\Theta}{\sqrt{\mathbf{C}\mathbf{N}_\Theta \cdot \mathbf{N}_\Theta}}(\mathbf{N}_\Theta \otimes \mathbf{N}_\Theta) - p^*\mathbf{C}^{-1}. \tag{21}$$

Recalling the definitions of $\mathbf{S}=\mathbf{J}\ \mathbf{F}^{-1}\boldsymbol{\sigma}\mathbf{F}^{-\mathrm{T}}$ and $\mathbf{C}=\mathbf{F}^{\mathrm{T}}\mathbf{F}$, Eq. (21) can be written in terms of the Cauchy stress tensor $\boldsymbol{\sigma}$,

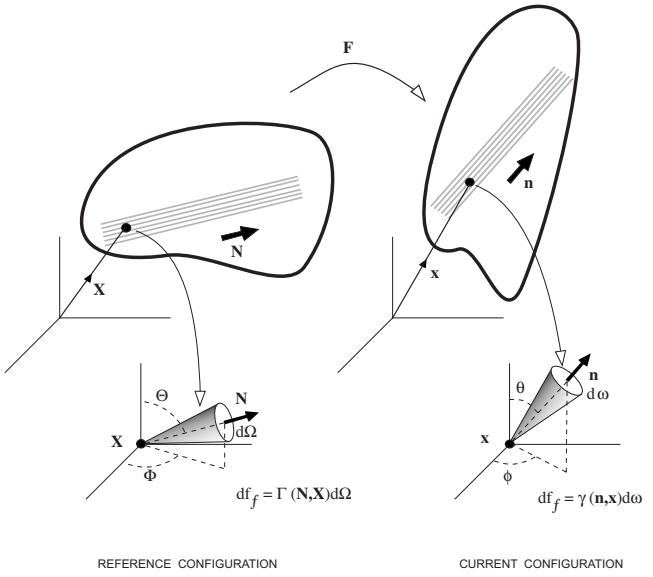

FIG. 2. Orientation of microfibrils in the reference and current configurations and solid angles.

$$\boldsymbol{\sigma} = \sum_\Theta \frac{f_f^\Theta s_f^\Theta}{|\mathbf{F}\mathbf{N}_\Theta|}(\mathbf{F}\mathbf{N}_\Theta \otimes \mathbf{F}\mathbf{N}_\Theta) - p^*\mathbf{I}, \tag{22}$$

where use has been made of incompressibility $J=1$ and the fact that the elongation in the microfibril,

$$\lambda_f^\Theta = \sqrt{\mathbf{C}\mathbf{N}_\Theta \cdot \mathbf{N}_\Theta} = \sqrt{\mathbf{F}^T\mathbf{F}\mathbf{N}_\Theta \cdot \mathbf{N}_\Theta} = \sqrt{\mathbf{F}\mathbf{N}_\Theta \cdot \mathbf{F}\mathbf{N}_\Theta} = |\mathbf{F}\mathbf{N}_\Theta|, \tag{23}$$

is the norm of the vector $\mathbf{F}\mathbf{N}_\Theta$.

Taking deviators in Eq. (22) and rearranging terms, the solution for the Cauchy stress for incompressible materials is

$$\boldsymbol{\sigma} = \sum_\Theta f_f^\Theta s_f^\Theta \left[\frac{\mathbf{F}\mathbf{N}_\Theta \otimes \mathbf{F}\mathbf{N}_\Theta}{|\mathbf{F}\mathbf{N}_\Theta|} - \frac{1}{3}|\mathbf{F}\mathbf{N}_\Theta|\mathbf{I}\right] - p\mathbf{I}, \tag{24}$$

which in combination with Eq. (17) completely defines the model. It is worth noting that p in Eq. (24) now represents the *total* hydrostatic pressure and has to be calculated from boundary conditions and/or equilibrium.

Use of Eqs. (16) and (24) in a given problem assumes knowledge of the specific fiber distribution and orientation across the material in the reference configuration. This is accomplished through the spatial distribution function $\Gamma(\mathbf{N},\mathbf{X})$, which can be defined as the volume fraction of microfibrils per unit solid angle having the direction $\mathbf{N}$ at a given position $\mathbf{X}$ in the reference configuration (Fig. 2). Therefore, the fraction of microfibrils in the solid angle $d\Omega$ around $\mathbf{N}$ at a given position $\mathbf{X}$ will be equal to

$$df_f = \Gamma(\mathbf{N},\mathbf{X})d\Omega. \tag{25}$$

The total volume fraction f_f at point $\mathbf{X}$ is obtained by integration of Eq. (25) over all the directions: i.e.,

$$f_f(\mathbf{X}) = \int_{1/2\ space} \Gamma(\mathbf{N},\mathbf{X}) d\Omega, \tag{26}$$

where we have arbitrarily assigned to the microfibrils a positive orientation with $\mathbf{N}\cdot\mathbf{e}_1 > 0$, $\mathbf{e}_1$ being the unit vector in the direction of the x_1 axis (Fig. 2), and performed the integral over the upper half-space.

Therefore, the continuous counterpart of the discrete equation (24) to compute Cauchy stress from the distribution of microfibrils is

$$\boldsymbol{\sigma}(\mathbf{X}) = \int_{1/2\ space} s_f \left[\frac{\mathbf{FN} \otimes \mathbf{FN}}{|\mathbf{FN}|} - \frac{1}{3}|\mathbf{FN}|\mathbf{I} \right] \Gamma(\mathbf{N},\mathbf{X}) d\Omega - p\mathbf{I}. \tag{27}$$

In the case that there is only one set of microfibrils, Γ takes the form of a Dirac delta function. If microfibrils are lined up along the x_1 axis, Γ can be expressed as

$$\Gamma = f_f \frac{\delta(\Theta)}{2\pi \sin\Theta}, \tag{28}$$

$\delta(\Theta)$ being the unidimensional delta function and Θ the angle between $\mathbf{N}$ and $\mathbf{e}_1$.

As deformation develops in the solid, microfibrils progressively align and change their orientation. The relationship between the reference orientation, defined by $\mathbf{N}$, and the current orientation $\mathbf{n}$ is given by

$$\mathbf{n} = \frac{\mathbf{FN}}{|\mathbf{FN}|}, \tag{29}$$

since $\mathbf{n}$ is the unit vector of the transformed direction $\mathbf{F}$ $\mathbf{N}$.

In the current configuration (Fig. 2), the fraction of microfibrils in the solid angle $d\omega$ around the unit vector $\mathbf{n}$ is equal to

$$df_f = \gamma(\mathbf{n},\mathbf{x}) d\omega, \tag{30}$$

$\gamma(\mathbf{n},\mathbf{x})$ being the spatial distribution function in the current configuration.

The function γ is related to Γ by

$$\gamma(\mathbf{n},\mathbf{x}) = |\mathbf{FN}_\Theta|^{3/2} \Gamma(\mathbf{N},\mathbf{X}), \tag{31}$$

which is obtained by identifying Eqs. (25) and (30) and using the relationship between the solid angles in the reference and current configurations with $J=1$.

The degree of orientation of microfibrils at a given time is characterized by the orientation index β, which measures the mean instant alignment with respect to a constant direction. The orientation index with reference to the x_1 axis is defined as

$$\beta(\mathbf{x}) = \frac{\int \gamma(\mathbf{n},\mathbf{x}) \mathbf{n}\cdot\mathbf{e}_1 d\omega}{\int \gamma(\mathbf{n},\mathbf{x}) d\omega} = \frac{1}{f_f} \int \gamma(\mathbf{n},\mathbf{x}) \mathbf{n}\cdot\mathbf{e}_1 d\omega, \tag{32}$$

where, as usual, the integrals in the solid angle are extended to the upper half-space. The orientation index can be interpreted as the ratio between the projected length of microfibrils along x_1 and their total length at a given instant.

The orientation index can be written as a function of Γ using Eqs. (25), (29), and (30): namely,

$$\beta(\mathbf{X}) = \frac{1}{f_f} \int \frac{\Gamma(\mathbf{N},\mathbf{X}) \mathbf{FN}\cdot\mathbf{e}_1}{|\mathbf{FN}|} d\Omega, \tag{33}$$

where only values in the reference configuration are considered.

Since we have considered only microfibrils with $\mathbf{N}\cdot\mathbf{e}_1 > 0$, Eqs. (32) and (33) do not give $\beta=0$ for the isotropic case—Γ (or γ)=const—but instead a value $\beta=\frac{1}{2}$ is obtained. When microfibrils are perfectly aligned ($\mathbf{n}\cdot\mathbf{e}_1=1$) the orientation index equals unity.

IV. APPLICATION TO TENSILE STRETCHING OF SILK FIBERS

The continuum model described above is specially suited for modeling biological fibers since it is able to capture the anisotropy, strong nonlinearity, and hierarchy exhibited by these materials due to the presence of a network of microfibrils embedded in a highly compliant matrix [16]. The model naturally links the mechanical response with the degree of internal orientation and, like other continuum models, it can be easily implemented in numerical programs. As an exemplification of its capabilities, this section shows a simulation of the effect of internal alignment on the tensile properties of spider dragline silk fibers.

Spider dragline silk or MAS, as it is usually labeled after the gland where it is produced—Major Ampullate—shows a striking combination of tensile strength and elongation at breaking that has fostered a great deal of research work to unravel its basis and to mimic such outstanding properties in biomimetic replicas [23–28]. MAS fibers are composed of amorphous flexible chains strongly hydrogen bonded, reinforced by crystallites [29], and their tensile behavior is highly determined by the network of hydrogen bonds and the degree of molecular orientation, as has been demonstrated by the authors elsewhere [30]. Whereas MAS fibers tested in air behave as glassy polymers due to hydrogen bonding [31], fibers tested in water show an elastomeric behavior as the result of water molecules disrupting the network of hydrogen bonds [32]. Stretching leads to an extension of a network of protein chains and a rotation of microcrystallites, and induces a net molecular alignment parallel to the fiber axis [29,33]. The authors have shown that deformation of MAS silk essentially takes place under conditions of volume constancy [34].

Until now, very few models have been developed for MAS fibers, all of them resorting to a detailed microstructural description in terms of a large number of parameters whose determination is very elusive [31]. Here we present a first attempt to develop a model for spider silk that, despite its macroscopic nature, keeps track of the internal alignment and other microstructural features.

In the following we assume that the fiber is *homogeneous and transversally isotropic*—i.e., that its properties are invariant along directions perpendicular to the fiber axis—and

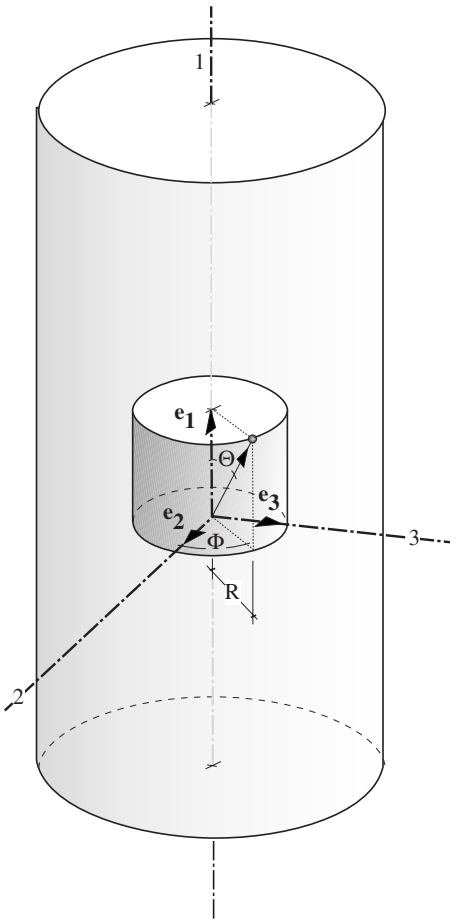

FIG. 3. Coordinate system for the macrofiber.

that it is axially loaded. Taking for convenience a Cartesian coordinate system whose x_1 axis is aligned with the fiber (Fig. 3), the unit vector $\mathbf{N}$ characterizing the initial orientation of microfibrils is written as

$$\mathbf{N} = \cos\Theta\mathbf{e}_1 + \sin\Theta\cos\Phi\mathbf{e}_2 + \sin\Theta\sin\Phi\mathbf{e}_3. \quad (34)$$

According to the hypotheses above, the distribution function $\Gamma(\mathbf{N},\mathbf{X})$ will only be a function of the polar angle Θ with respect to the symmetry axis and independent of the azimuthal angle Φ and the position $\mathbf{X}$.

Due to symmetry, the Cauchy stress tensor at any point of the fiber is

$$\sigma = \begin{bmatrix} \sigma & 0 & 0 \\ 0 & 0 & 0 \\ 0 & 0 & 0 \end{bmatrix}, \quad (35)$$

σ being the true tensile stress, defined as

$$\sigma = \frac{T}{a}, \quad (36)$$

where T is force applied and a the current cross-sectional area of the fiber.

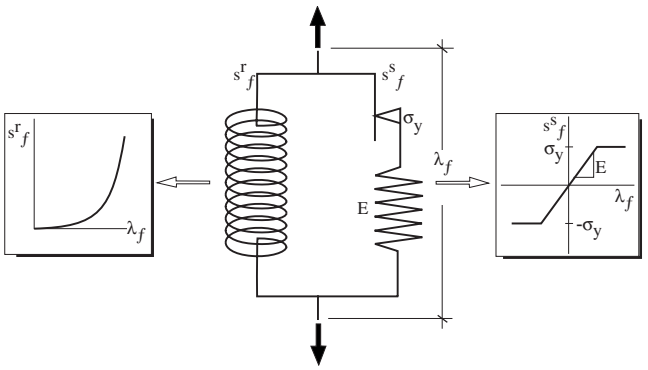

FIG. 4. Analogical model for the microfibrils.

The components of the deformation gradient tensor $\mathbf{F}$ are

$$\mathbf{F} = \begin{bmatrix} \lambda & 0 & 0 \\ 0 & 1/\sqrt{\lambda} & 0 \\ 0 & 0 & 1/\sqrt{\lambda} \end{bmatrix}, \quad (37)$$

where λ is the axial stretching of the fiber. Note that like the stress tensor, $\mathbf{F}$ does not depend on the point considered and that $\det\mathbf{F}=1$, as required by incompressibility [34]. Equations (35) and (37) show that this simple problem is mechanically determined by only two macroscopic external parameters: namely, the tensile true stress σ and the axial stretching λ.

The link between σ and λ is established via the constitutive equation determined by expression (27) and the relationship between the stress and the deformation in the microfibrils, Eq. (17), for which a simple analogical model is postulated, capturing the well-known behavior of spider silks (Fig. 4); a nonlinear spring representing the stretching and orientation of molecular chains in the rubbery state (i.e., with the network of hydrogen bonds deactivated), in parallel with a skidding block with a linear spring to account for the breaking of hydrogen bonds and molecular slippage when the fiber is over the glass transition.

The nominal stress due to the nonlinear spring can be written as

$$s_f^r = K(1-\lambda_f)^4, \quad (38)$$

which provides a good approximation to the elastomeric behavior of spider silk for $\lambda_f < 3$. The conditions where spider silk behaves elastomerically have been determined by the authors and can be found elsewhere [35].

Molecular slippage and breaking of hydrogen bonds over the glass transition is simulated by the use of a skidding block with stress threshold σ_y in series with a linear spring with elastic modulus E. The total nominal stress in the microfibril, s_f, will be the sum of the stress due to the stretching and orientation of molecular chains, s_f^r plus the stress due to slippage and hydrogen bond breaking, s_f^s.

$$s_f = s_f^r + s_f^s. \quad (39)$$

Use of Eqs. (34) and (37) yields a tensor $\mathbf{FN}\otimes\mathbf{FN}$ equal to

$$\mathbf{FN} \otimes \mathbf{FN} = \begin{bmatrix} \lambda^2 \cos^2\Theta & \frac{\sqrt{\lambda}}{2}\sin 2\Theta \cos\Phi & \frac{\sqrt{\lambda}}{2}\sin 2\Theta \sin\Phi \\ \frac{\sqrt{\lambda}}{2}\sin 2\Theta \cos\Phi & \frac{1}{\lambda}\sin^2\Theta \cos^2\Phi & \frac{1}{2\lambda}\sin^2\Theta \sin 2\Phi \\ \frac{\sqrt{\lambda}}{2}\sin 2\Theta \sin\Phi & \frac{1}{2\lambda}\sin^2\Theta \sin 2\Phi & \frac{1}{\lambda}\sin^2\Theta \sin^2\Phi \end{bmatrix}, \quad (40)$$

while the elongation in the microfibril λ_f results in

$$\lambda_f = |\mathbf{FN}| = \sqrt{\lambda^2 \cos^2\Theta + \frac{1}{\lambda}\sin^2\Theta}. \quad (41)$$

The tensile stress σ is obtained by substituting Eqs. (39) and (40) into Eq. (27),

$$\sigma = \int_0^{\pi/2} \frac{\pi(s_f^r + s_f^r)\Gamma(\Theta)}{\sqrt{\lambda^2 \cos^2\Theta + \frac{1}{\lambda}\sin^2\Theta}} \times \left(2\lambda^2 \cos^2\Theta - \frac{1}{\lambda}\sin^2\Theta\right)\sin\Theta d\Theta, \quad (42)$$

where $d\Omega = 2\pi \sin\Theta d\Theta$ and the integral is evaluated only in the upper half-space.

The orientation index, Eq. (33), now reads

$$\beta = \frac{2\pi}{f_f}\int_0^{\pi/2} \Gamma(\Theta)\frac{\lambda \cos\Theta \sin\Theta}{\sqrt{\lambda^2 \cos^2\Theta + \frac{1}{\lambda}\sin^2\Theta}} d\Theta. \quad (43)$$

Figure 5 shows the experimental results of tensile tests performed in air of MAS fibers with three different degrees of molecular alignment which were obtained as described elsewhere [30]. Briefly, samples were submerged in water and allowed to contract up to the supercontracted length L_{SC}. Then fibers were stretched up to the selected initial length L_C and allowed to dry. The alignment parameter α is used to control the process and is defined as

$$\alpha = \frac{L_C}{L_{SC}} - 1. \quad (44)$$

Dried supercontracted fibers ($\alpha=0$) are in their most disordered molecular state and have been considered isotropic.

Figure 5 also presents the result of numerical computations for the three kinds of MAS fibers, where the mi-

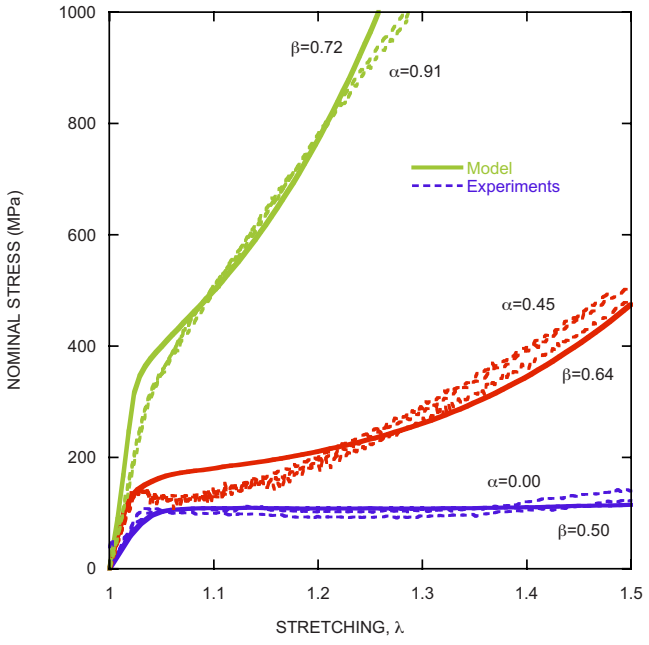

FIG. 5. (Color online) Tensile curves of MAS fiber with different alignments. Model results are labeled by the orientation index β [Eq. (43)]. Experimental data are identified by alignment parameter α [Eq. (44)].

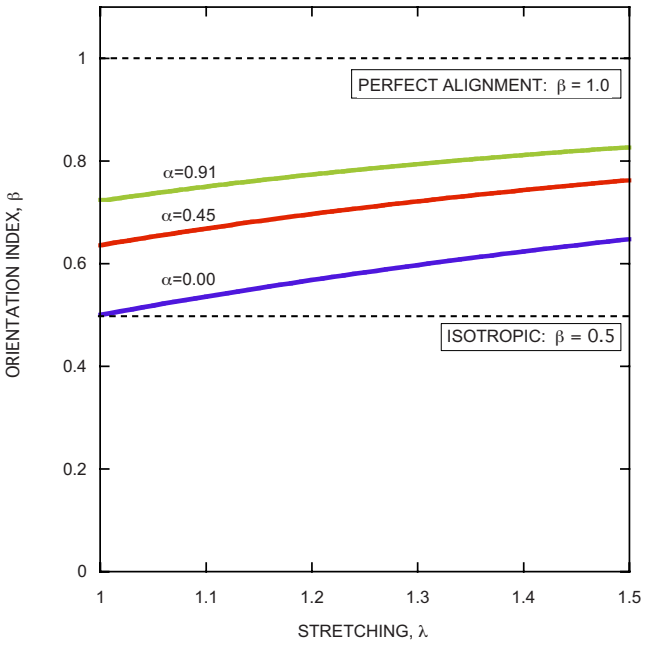

FIG. 6. (Color online) Variation of the orientation index β [Eq. (43)] with tensile stretching. Curves corresponding to samples with different initial molecular alignments are labeled by their initial alignment parameter α [Eq. (44)].

crofibrils were modeled using the analogical model shown in Fig. 4 with $K=1000$ MPa, $\sigma_y=300$ MPa, and $E=15$ GPa. Only two (σ_y and E) of the required parameters were obtained by fitting to the tensile curves in Fig. 5, whereas Eq. (38) had been previously determined from the elastomeric behavior of MAS silk. A volume fraction of fibers, $f_f=1$, was assumed in all cases. Nominal stresses were computed by dividing the tensile load by the cross-sectional area at the beginning of the test. For each curve, the value of the orientation index β is also shown, computed before stretching the samples.

Whereas isotropic MAS fibers ($\alpha=0$) were modeled with a constant value of the distribution function of microfibrils $\Gamma=f_f/2\pi$, tensile curves of oriented fibers ($\alpha=0.45$ and $\alpha=0.90$) were obtained from isotropic ones by a process resembling the experimental procedure: First, the isotropic fiber ($\Gamma=f_f/2\pi$) is stretched up to the selected alignment—i.e., $\lambda=1.45$ or 1.90—while keeping the skidding blocks disengaged (by setting $\sigma_y=0$). This process simulates stretching in water where the hydrogen bonds are deactivated by water molecules. Then, the skidding blocks are activated (restoration of hydrogen bonds upon drying) and the fiber is unloaded. Finally, the fiber is loaded again, taking the length and cross-sectional area at the beginning of this stage as reference values for computing stress and strain.

As shown in Fig. 5, the agreement between experiments and simulation is remarkable, especially taking into account that the numerical modeling reproduces the experimental procedure step by step. The proposed model is able to follow the large deformation of MAS fibers and properly captures their alignment process, easily incorporating the main operative microstructural mechanisms.

In addition, the model gives valuable information, such as of the orientation index β—Eq. (43)—which can be useful in linking macroscopic parameters like the alignment parameter α with the internal distribution of microfibrils. Figure 6 shows the evolution of the orientation index β with the applied stretching λ for the three selected initial alignments $\alpha=0$, 0.45, and 0.91, corresponding to $\beta=0.5$, 0.64, and 0.72. The orientation index monotonically increases with λ, although this increment reduces progressively as the sample is stretched. After a given stretching, the greater increments in β are obtained for isotropic fibers, whereas highly oriented samples show the lowest increases in orientation. Ideally, the perfect alignment state $\beta=1$ would be reached asymptotically for λ tending to infinity. Nevertheless, the tensile strength of MAS silk imposes a practical limit of about 0.9 for orientation indexes obtained by stretching.

ACKNOWLEDGMENTS

This work was funded by Ministerio de Ciencia y Tecnología (Spain) through Projects Nos. MAT2005-06320 and MAT2006-4387 and by Comunidad de Madrid through Programs Nos. ESTRUMAT/S-0505/MAT/000077, DUMEINPA/S-0505/MAT/000155, and MADR.IB-CM/S-SAL/0312/2006.

[1] L. R. G. Treloar, *The Physics of Rubber Elasticity* (Clarendon, Oxford, 1958).
[2] O. Kratky and G. Porod, Recl. Trav. Chim. Pays-Bas **68**, 1106 (1949).
[3] H. M. James and E. Guth, J. Chem. Phys. **11**, 455 (1943).
[4] E. M. Arruda and M. C. Boyce, J. Mech. Phys. Solids **41**, 389 (1993).
[5] P. D. Wu and E. van der Giessen, J. Mech. Phys. Solids **41**, 427 (1993).
[6] J. J. M. Baltussen and M. G. Northolt, Polymer **40**, 6113 (1999).
[7] H. J. Ji, C. Ortiz, and M. C. Boyce, ASME J. Eng. Mater. Technol. **128**, 509 (2006).
[8] H. Zhou and Y. Zhang, Phys. Rev. Lett. **94**, 028104 (2005).
[9] Y. C. Fung, *Biomechanics: Mechanical Properties of Living Tissues*, 2nd ed. (Springer, New York, 1993).
[10] J. D. Humprey, *Cardiovascular Solid Mechanics* (Springer, New York, 2002).
[11] G. A. Holzapfel, T. C. Gasser, and R. W. Ogden, J. Elast. **61**, 1 (2000).
[12] A. J. M. Spencer, in *Continuum Theory of the Mechanics of Fibre-reinforced Composites*, edited by A. J. M. Spencer *et al.*, CISM Course No. 282 (Springer, New York, 1984).
[13] Y. Termonia, Macromolecules **27**, 7378 (1994).
[14] D. Porter, F. Vollrath, and Z. Shao, Eur. Phys. J. E **16**, 199 (2005).
[15] *Silk Polymers*, edited by D. Kaplan *et al.*, ACS Symposium Series No. 544 (ACS, Washington D. C., 1994).
[16] *Structural Biological Materials*, edited by M. Elices (Pergamon, Amsterdam, 2000).
[17] P. Chadwick, *Continuum Mechanics: Concise Theory and Problems* (Dover, Mineola, NY, 1999).
[18] R. Hill, J. Mech. Phys. Solids **13**, 213 (1965).
[19] J. Mandel, in *Plasticite Classique et Viscoplasticite*, CISM Course No. 97 (Springer, Berlin 1972).
[20] R. J. Swenson, Am. J. Phys. **51**, 940 (1983).
[21] D. N. Theodorou, T. D. Boone, L. R. Dodd, and K. F. Mansfield, Makromol. Chem., Theory Simul. **2**, 191 (1993).
[22] R. G. Winkler, J. Chem. Phys. **117**, 2449 (2002).
[23] M. Elices, J. Pérez-Rigueiro, G. R. Plaza, and G. V. Guinea, J. Appl. Polym. Sci. **92**, 3537 (2004).
[24] M. Elices, J. Pérez-Rigueiro, G. R. Plaza, and G. V. Guinea, J. Test. Eval. **2005**, 60 (2005).
[25] M. Elices, G. V. Guinea, G. R. Plaza, J. I. Real, and J. Pérez-Rigueiro, J. Mater. Res. **21**, 1931 (2006).
[26] J. M. Gosline, M. Lillie, E. Carrington, P. A. Guerette, C. S. Ortlepp, and K. N. Savage, Philos. Trans. R. Soc. London, Ser. B **357**, 121 (2002).
[27] D. P. Knight and F. Vollrath, Philos. Trans. R. Soc. London, Ser. B **357**, 155 (2002).
[28] F. Vollrath, Rev. Mol. Biotechnol. **74**, 67 (2000).
[29] J. M. Gosline, P. A. Guerette, C. S. Ortlepp, and K. N. Savage,

J. Exp. Biol. **202**, 3295 (1999).
[30] G. V. Guinea, M. Elices, J. Pérez-Rigueiro, and G. R. Plaza, J. Exp. Biol. **208**, 25 (2005).
[31] Y. Termonia, in *Structural Biological Materials*, edited by M. Elices (Pergamon Press, Amsterdam, 2000), p. 335.
[32] J. M. Gosline, M. Denny, and M. E. DeMont, Nature (London) **309**, 551 (1984).
[33] D. T. Grubb and J. Gending, Int. J. Biol. Macromol. **24**, 203 (1999).
[34] G. V. Guinea, J. Pérez-Rigueiro, G. R. Plaza, and M. Elices, Biomacromolecules **7**, 2173 (2006).
[35] G. R. Plaza, G. V. Guinea, J. Pérez-Rigueiro, and M. Elices, J. Polym. Sci., Part B: Polym. Phys. **44**, 994 (2006).